

Emery–Dreifuss muscular dystrophy–linked genes and centronuclear myopathy–linked genes regulate myonuclear movement by distinct mechanisms

Mary Ann Collins[†], Torrey R. Mandigo[†], Jaclyn M. Camuglia, Gabriella A. Vazquez, Alyssa J. Anderson, Christine H. Hudson, John L. Hanron, and Eric S. Folker*
Biology Department, Boston College, Chestnut Hill, MA 02467

ABSTRACT Muscle cells are a syncytium in which the many nuclei are positioned to maximize the distance between adjacent nuclei. Although mispositioned nuclei are correlated with many muscle disorders, it is not known whether this common phenotype is the result of a common mechanism. To answer this question, we disrupted the expression of genes linked to Emery–Dreifuss muscular dystrophy (EDMD) and centronuclear myopathy (CNM) in *Drosophila* and evaluated the position of the nuclei. We found that the genes linked to EDMD and CNM were each necessary to properly position nuclei. However, the specific phenotypes were different. EDMD-linked genes were necessary for the initial separation of nuclei into distinct clusters, suggesting that these factors relieve interactions between nuclei. CNM-linked genes were necessary to maintain the nuclei within clusters as they moved toward the muscle ends, suggesting that these factors were necessary to maintain interactions between nuclei. Together these data suggest that nuclear position is disrupted by distinct mechanisms in EDMD and CNM.

Monitoring Editor
Robert D. Goldman
Northwestern University

Received: Oct 18, 2016
Revised: Apr 27, 2017
Accepted: Jun 14, 2017

INTRODUCTION

Based on their abundance and their repetitive structure, myofibers—the cellular units of skeletal muscle—have long been a model system to identify cell-biological mechanisms that underlie development. Many features of myofiber structure, however, such as their syncytial nature, are specialized for muscle cells. During the development of an individual muscle cell, many mononucleated myoblasts fuse to form a syncytial myofiber that can contain up to

thousands of nuclei (Kim *et al.*, 2015), each of which is precisely positioned. Most nuclei are distributed evenly throughout the muscle, with a small cluster of nuclei associated with the neuromuscular junction (Bruusgaard *et al.*, 2004, 2006). Disruptions in the distribution of nuclei have been correlated with muscle disease for several decades (Dubowitz and Sewry, 2007). Two muscle diseases in which mispositioned nuclei are abundant are Emery–Dreifuss muscular dystrophy (EDMD) (Sewry *et al.*, 2001) and centronuclear myopathy (CNM) (Spiro *et al.*, 1966). It is not clear, however, whether the position of the nuclei is a consequence of ongoing muscle repair or mispositioned nuclei contribute to muscle weakness and muscle deterioration. More fundamentally, it is not known whether mispositioned nuclei in disparate muscle diseases arise from common or distinct mechanisms.

To determine whether mispositioned nuclei are the result of a common cellular disruption or are due to disease-specific cellular defects, we evaluated the position of nuclei in *Drosophila* that had disruptions in genes linked to EDMD or CNM. Each of the genes mutated in patients with EDMD encodes for a protein that is localized to the nucleoskeleton or the nuclear envelope (Meinke *et al.*, 2011). Based on this localization, the function of some EDMD-linked genes with respect to nuclear position has been tested in muscle (Zhang *et al.*, 2009; Dialynas *et al.*, 2010; Elhanany-Tamir *et al.*, 2012),

This article was published online ahead of print in MBoC in Press (<http://www.molbiolcell.org/cgi/doi/10.1091/mbc.E16-10-0721>) on June 21, 2017.

[†]These authors contributed equally to this work.

*Address correspondence to: Eric S. Folker (eric.folker@bc.edu).

Abbreviations used: AEL, after egg lay; *Amph*, amphiphysin; *apRed*, apterous red; *bocks*, bocksbeutel; CNM, centronuclear myopathy; *Dhc*, dynein heavy chain; EDMD, Emery–Dreifuss muscular dystrophy; *Khc*, kinesin heavy chain; *klar*, klarsicht; *koi*, klaroid; L1, 1st instar larval stage; L3, 3rd instar larval stage; LINC complex, linker of nucleoskeleton and cytoskeleton; LT, lateral transverse; *mtm*, myotubularin; *Ote*, otefin; RNAi, RNA interference; RT-PCR, reverse transcriptase PCR; SUN, Sad1 and Unc84 homology domain; VL3, ventral longitudinal muscle 3.

© 2017 Collins, Mandigo, *et al.* This article is distributed by The American Society for Cell Biology under license from the author(s). Two months after publication it is available to the public under an Attribution–Noncommercial–Share Alike 3.0 Unported Creative Commons License (<http://creativecommons.org/licenses/by-nc-sa/3.0>).

“ASCB[®],” “The American Society for Cell Biology[®],” and “Molecular Biology of the Cell[®]” are registered trademarks of The American Society for Cell Biology.

cultures of myoblast-derived cells (Cadot et al., 2012; Wilson and Holzbaur, 2014), and other cell types (Gundersen and Worman, 2013).

In mammals, *SYNE1* and *SYNE2* are necessary for the clustering of nuclei at the postsynaptic side of the neuromuscular junction (Q. Zhang et al., 2007; J. Zhang et al., 2009). Furthermore, nesprin proteins and SUN proteins regulate the distribution of nuclei throughout the muscle in *Drosophila* embryos and larvae (Elhanany-Tamir et al., 2012) and in mammalian cell culture systems (Wilson and Holzbaur, 2014). In addition, emerin is essential for nuclear movement during cell migration (Chang et al., 2013). However, these experiments were all completed in different systems, making it difficult to compare the functions of each factor with respect to nuclear movement during muscle development in vivo.

Despite the name centronuclear myopathy, there has been little investigation of the causes or consequences of mispositioned nuclei with respect to CNM. The genes mutated in patients with CNM encode for proteins that regulate the development and structure of the T-tubule in skeletal muscle or the release of calcium in skeletal muscle (Jungbluth et al., 2007). Therefore it is believed that defects in Ca^{2+} signaling and T-tubule structure underlie CNM. However, we recently demonstrated that the movement of nuclei in muscle is an early event in muscle development that precedes myofibril assembly (Auld and Folker, 2016) and therefore precedes a fully developed T-tubule network (Flucher et al., 1993).

Furthermore, it was recently demonstrated that the proteins linked to CNM have additional cellular functions. Specifically, amphiphysin-dependent activation of N-WASP was demonstrated to be a prerequisite for triad formation (the junction between the T-tubules and the sarcoplasmic reticulum) and was necessary for proper movement of nuclei to the periphery of a cultured myofiber system (Falcone et al., 2014). In addition, amphiphysin contributed to the attachment between the nucleus and the cytoskeleton and nuclear movement in culture (D'Alessandro et al., 2015). The latter function suggests that nuclear position may be regulated by the concerted actions of amphiphysin (and perhaps other CNM-linked genes) and the proteins linked to EDMD that localize to the nucleus.

We compared the effects of genes linked to CNM and EDMD during muscle development in *Drosophila* embryos and larvae. This system combines a short developmental timeline with optical clarity and rich genetic resources, which made it possible to measure the precise distribution of nuclei at different developmental stages. Consistent with previous reports (Elhanany-Tamir et al., 2012), the LINC complex, which has been linked to EDMD, contributed to myonuclear positioning in both the embryo and the larva. In addition, the CNM-linked genes *Amphiphysin* (*Amph*) and *myotubularin* (*mtm*) are also necessary for positioning myonuclei in both the embryo and the larva. However, the effects of the CNM-linked genes were milder and are mechanistically distinct. CNM-linked genes and EDMD-linked genes exhibit different interactions with the microtubule motors dynein and kinesin. Furthermore, live-embryo time-lapse microscopy of myonuclear movement was used to demonstrate that the loss of *Amphiphysin* caused reduced interactions between nuclei, whereas the loss of *bocksbeutel* (*Drosophila* emerin) caused enhanced interactions between nuclei. Thus nuclear position is likely disrupted by distinct mechanisms in different muscle disorders.

RESULTS

Muscle function in *Drosophila* larvae requires genes mutated in patients with EDMD or CNM

To determine whether EDMD- and CNM-linked genes affect muscle function in *Drosophila*, we tested larval locomotion in larvae

from which *Otefin* (*Drosophila* emerin), *bocksbeutel* (*Drosophila* emerin), *klaroid* (*Drosophila* SUN), *klarsicht* (*Drosophila* nesprin), or *Amphiphysin* was zygotically removed with the respective *Ote*^{B279}, *bocks*^{DP01391}, *koi*^{HRKO80.w}, *klar*¹, or *Amph*²⁶ null alleles. The *bocks*^{DP01391}, *klar*¹, and *Amph*²⁶ homozygotes moved more slowly than their respective heterozygous and control larvae (Figure 1A). These data indicate that *bocksbeutel*, *klarsicht*, and *Amphiphysin* are all necessary for proper muscle function. Both *Ote*^{B279} and *koi*^{HRKO80.w} were homozygous lethal, and thus the effect of these alleles on animal movement could not be determined.

To determine whether the effect on muscle function was correlated with mispositioned nuclei, we measured the spacing of nuclei in *Drosophila* larvae. The distance between nuclei in *Drosophila* larvae has been measured in many studies (Elhanany-Tamir et al., 2012; Folker et al., 2012; Metzger et al., 2012; Schulman et al., 2014), but only rarely has the effect of muscle size been considered (Folker et al., 2012; Schulman et al., 2014), and never has the number of nuclei been considered. We measured the internuclear distance as a function of muscle size and the number of nuclei to determine how evenly nuclei were distributed (Figure 1 and Supplemental Figure S1).

In control larvae, the distribution of nuclei was consistent. In most muscles, nuclei were arranged in two lines parallel to the long axis of the muscle. Both control genotypes—*twist-GAL4*, *apRed* and *DMef2-GAL4*, *apRed*—had nearly identical internuclear distance ratios of 78% of maximal. In *bocks*^{DP01391} and *klar*¹ larvae, nuclei were in a single line positioned centrally within the muscle and parallel to the long axis of the muscle (Figure 1B). Quantitatively, the internuclear distance was 55% of maximal for both *bocks*^{DP01391} and *klar*¹ larvae (Figure 1C). In *Amph*²⁶ larvae, there were regions of single-file nuclei and regions with clusters of nuclei (Figure 1B). Quantitatively, in *Amph*²⁶ larvae, the internuclear distance was 64% of maximal (Figure 1C). Nuclear position was also measured relative to the muscle edge in each genotype. In *bocks*^{DP01391} and *klar*¹ larvae, nuclei were farther from the muscle edge than in controls (Figure 1D). However, nuclear position relative to the muscle edge was not affected in *Amph*²⁶ larvae. Finally, the distance between the two parallel lines was similar in *Amph*²⁶ and control larvae. However, this value was nearly zero in most *bocks*^{DP01391} and *klar*¹ larvae (Figure 1E). These data indicate that all three of *bocks*, *klar*, and *Amph* are necessary for proper nuclear positioning in larval muscle, but that the specific phenotype caused by the loss of *bocksbeutel* or *klarsicht* is different from the phenotype caused by the loss of *Amphiphysin*.

To determine whether the effect of each gene on nuclear position was muscle autonomous, we used the GAL4/UAS system to deplete each protein specifically from muscle. UAS-RNA interference (RNAi) expression, using RNAi lines that were validated by reverse transcriptase PCR (RT-PCR) (Supplemental Table S1), was driven from embryonic stage 12 through larval development under the control of *DMef2-GAL4*. RNAi experiments included another CNM-linked gene, *Myotubularin1* (*mtm*), which is mutated in some patients with a severe form of CNM (Liechti-Gallati et al., 1991). Muscle-specific depletion of either *bocks* or *klar* phenocopied the null larvae (*bocks*^{DP01931} and *klar*¹), as large regions of muscle had nuclei arranged in a single line rather than two parallel lines (Figure 2A), and the average internuclear distance was 63% of maximal (Figure 2B). Muscle-specific depletion of *koi* resembled *bocks*- and *klar*-depleted larvae in that nuclei formed a single line with an internuclear distance ratio of 68% of maximal (Figure 2, A and B). Muscle-specific depletion of *Ote* led to larvae with nuclei forming several clusters and an internuclear distance ratio of 68% of maximal

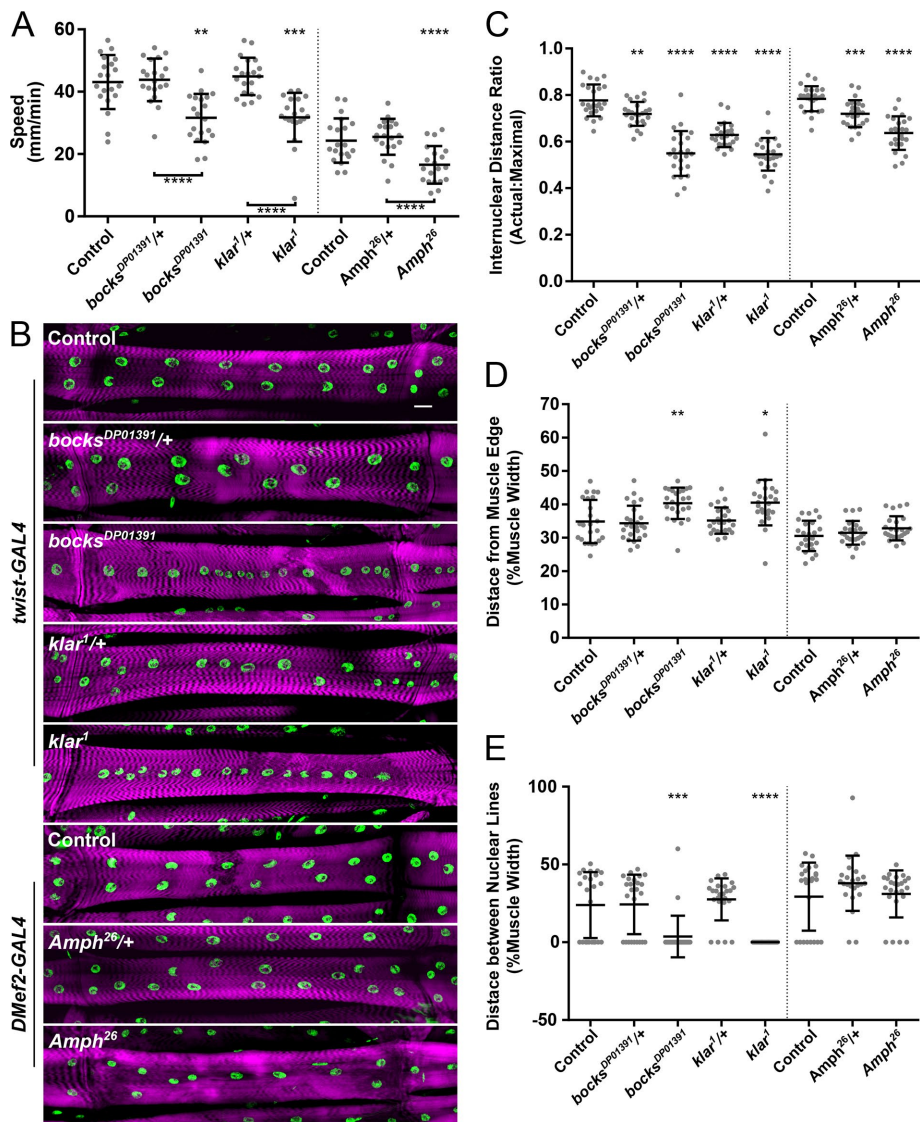


FIGURE 1: The EDMD-linked genes *bocksbeutel* and *klarsicht* and the CNM-linked gene *Amphiphysin* are necessary for proper locomotion and myonuclear position in *Drosophila* larvae. (A) The average speed of *Drosophila* larvae as they crawl toward an odorant stimulus. Error bars indicate SD from 20 larvae. It is important to note that the control genotype for the *Amph²⁶* larvae was different from that of *bocks^{DP01391}* and *klar¹* because there are slight phenotypic differences between *twist-GAL4*, *apRed* and *DMef2-GAL4*, *apRed* larvae. (B) Immunofluorescence images of VL3 muscles from dissected stage L3 larvae. The sarcomeres were stained with phalloidin (magenta), and the nuclei were stained with Hoechst (green). Scale bar, 25 μ m. (C) The ratio of actual internuclear distance to maximal internuclear distance in larval muscles from the indicated genotypes. Data points indicate the average value for the internuclear distance ratio for all nuclei within a single VL3 muscle. (D) The distance between nuclei and the nearest muscle edge in larval muscles from the indicated genotypes. Data points indicate the average distance from the muscle edge for all nuclei within a single VL3 muscle. (E) The distance between nuclear lines in larval muscles from the indicated genotypes. Data points indicate the average distance between distinct lines of nuclei within a single VL3 muscle. In C–E, error bars indicate SD from 24 VL3 muscles. Student's *t* test was used for comparison to controls. **p* < 0.05, ***p* < 0.005, ****p* < 0.0005, *****p* < 0.00005.

(Figure 2, A and B). Expression of *Amph* RNAi or *mtm* RNAi caused a milder phenotype (Figure 2A), with the evenness of nuclear positioning being 70 and 74% of maximal (Figure 2B). In addition, *DMef2-GAL4*-mediated depletion of each gene product, except for *mtm*, resulted in nuclei that were positioned farther from the muscle edge than with control (Figure 2C). The effects on the distance between

lines of nuclei were more complicated. Lines of nuclei were closer together when *koi* or *klar* was depleted, whereas lines of nuclei were farther apart when *mtm* was depleted than with controls (Figure 2D).

Because *DMef2-GAL4*-mediated expression of an RNAi in muscle begins at stage 12 of embryonic development and continues throughout larval development, we used *twist-GAL4* to acutely drive the expression of the RNAi earlier in development from stage 8 through stage 13 in the mesoderm. Thus, with this manipulation, the expression of each gene is disrupted only during a short and defined time period early in muscle development. *twist-GAL4*-mediated depletion of each gene phenocopied the *DMef2-GAL4*-mediated depletion with respect to the evenness of nuclear spacing (Supplemental Figure S2, A and B). However *twist-GAL4* mediated expression of RNAi against each gene did not affect the position of nuclei relative to the muscle edge (Supplemental Figure S2C) or the distance between lines of nuclei (Supplemental Figure S2D). These data suggest that the general distribution of nuclei throughout the muscle is regulated early in development but that additional regulation of the position of nuclei relative to the muscle edge occurs later.

To determine whether *bocksbeutel* and *Amphiphysin* are required only for the initial movement of nuclei or are also required to maintain nuclear positioning during larval development, expression of the *bocksbeutel* and *Amphiphysin* RNAi was driven under the control of *MHC-GAL4*, which drives expression of the RNAi later in development from the L1 larval stage throughout adulthood. *MHC-GAL4*-mediated depletion of *bocksbeutel* or *Amphiphysin* resulted in a disruption of nuclear positioning throughout the muscle (Supplemental Figure S3, A and B). In addition, depletion of either *bocksbeutel* or *Amphiphysin* affected the distance between lines of nuclei producing either nuclear lines that were closer together or no discernible nuclear lines (Supplemental Figure S3D). However only depletion of *Amphiphysin* disrupted the position of nuclei relative to the muscle edge (Supplemental Figure S3C). These data suggest that both *bocksbeutel* and *Amphiphysin* are required during larval development to maintain nuclear positioning within larval muscles.

Disruption of EDMD- and CNM-linked genes affects nuclear position in the *Drosophila* embryo

Because *twist-GAL4*-mediated depletion of each gene affected nuclear position in larvae, we next sought to understand the function of each gene during embryonic myonuclear movement. During embryonic muscle development in *Drosophila*, the nuclei undergo a

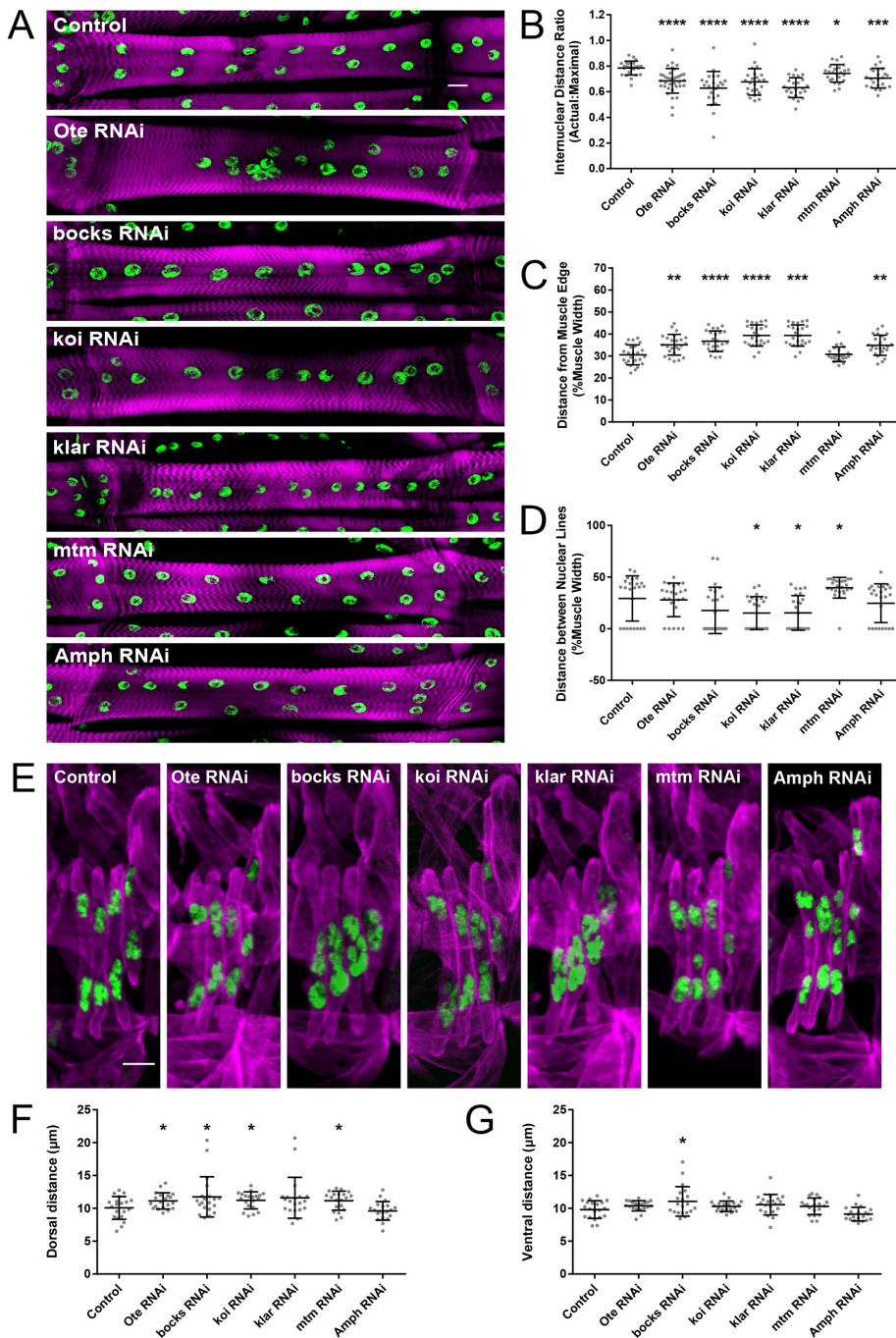


FIGURE 2: The effects of *bocksbeutel*, *klarsicht*, and *Amphiphysin* on nuclear position in larval and embryonic muscles are muscle autonomous. (A) Immunofluorescence images of VL3 muscles from stage L3 larvae that expressed RNAi against the indicated gene under the control of the muscle-specific driver *DMef2-GAL4*. The sarcomeres were stained with phalloidin (magenta), and the nuclei were stained with Hoechst (green). Scale bar, 25 μm . (B) Ratio of actual internuclear distance to maximal internuclear distance in larval muscles that expressed the indicated UAS-RNAi constructs under the control of the muscle-specific driver *DMef2-GAL4*. Data points indicate the average value for all nuclei within a single VL3 muscle. (C) Distance between nuclei and the nearest muscle edge in larvae that expressed the indicated UAS-RNAi constructs under the control of *DMef2-GAL4*. Data points indicate the average distance from the muscle edge of all nuclei within a single VL3 muscle. (D) Distance between nuclear lines in larval muscles from larvae that expressed the indicated UAS-RNAi constructs under the control of *DMef2-GAL4*. Data points indicate the average distance between nuclear lines within a single VL3 muscle. In B–D, error bars indicate SD from 24 VL3 muscles. (E) Immunofluorescence images of LT muscles in one hemisegment from stage 16 (16 h AEL) embryos that expressed the indicated UAS-RNAi constructs under the control of *DMef2-GAL4*. Embryos are oriented such that top is dorsal, bottom is ventral, left is anterior, and right is posterior. Muscles are identified by tropomyosin

complex set of movements, which involve 1) the separation of nuclei into two distinct clusters, 2) the directed movement of these clusters toward their respective ends of the muscle, and 3) the dispersion of nuclei throughout the muscle. To determine whether genes that have been linked to EDMD and CNM contribute to the active movement of nuclei during embryonic development, we measured the position of nuclei in the lateral transverse (LT) muscles of stage 16 (16 h after egg lay [AEL]) embryos as previously described (Folker *et al.*, 2012). In control embryos, the nuclei in each LT muscle were positioned in two separate clusters, with one near the dorsal end of the muscle and the other near the ventral end of the muscle (Figure 2E).

The *GAL4/UAS* system was used to deplete each EDMD- and CNM-linked protein to test for muscle-autonomous effects. *DMef2-GAL4*-mediated depletion of *Ote*, *bocks*, or *koi* caused an increase in the distance between the dorsal end of the muscle and the nearest nucleus in each genotype (Figure 2, E–G). Across the entire population, depletion of *klar* did not affect the average position of nuclei. However, 20% of LT muscles in *klar*- and *bocks*-depleted embryos had all of their nuclei positioned near the ventral end of the muscle. In addition, expression of RNAi against *klar* driven earlier in development by *twist-GAL4* did cause a statistical difference in the position of nuclei in the embryo (Supplemental Figure S2, E–G). These data indicate that the effects of *klar*, *bocks*, *Ote*, and *koi* on nuclear position are muscle autonomous and occur during embryonic development. In contrast, *DMef2-GAL4*-driven expression of *mtm* RNAi caused only a mild mispositioning of the nuclei relative to the ventral end of the muscle (Figure 2G), and RNAi against *Amph* had no effect on the position of myonuclei (Figure 2, E–G). Together

immunostaining (magenta), and the nuclei of the LT muscles are identified by DsRed immunostaining (green). Scale bars, 10 μm . (F, G) Distance between the dorsal end of the muscle and the nearest nucleus (F) and between the ventral end of LT muscles and the nearest nucleus (G) in embryos that expressed the indicated UAS-RNAi constructs driven with *DMef2-GAL4*. For F and G, each data point indicates the average distance within a single embryo. Error bars indicate SD from 20 embryos. Student's *t* test was used for comparison to controls. * $p < 0.05$, ** $p < 0.005$, *** $p < 0.0005$, **** $p < 0.00005$.

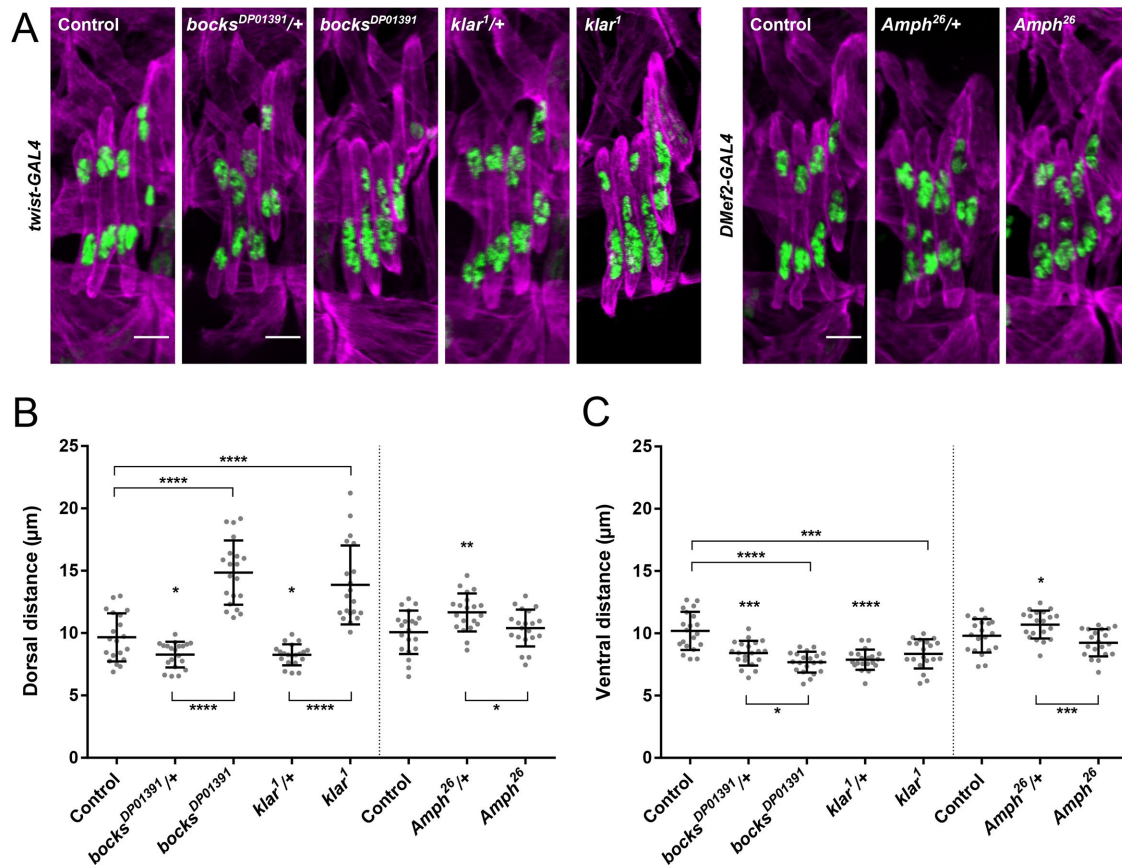


FIGURE 3: *Bocksbeutel*, *klarsicht*, and *Amphiphysin* are necessary for proper myonuclear position in *Drosophila* embryos. (A) Immunofluorescence images of LT muscles in one hemisegment from stage 16 (16 h AEL) embryos with the indicated genotypes. All embryos also carry either *twist-GAL4*, *apRed* or *DMef2-GAL4*, *apRed* for the identification of nuclei. Embryos are oriented such that top is dorsal, bottom is ventral, left is anterior, and right is posterior. Muscles were identified by immunostaining for tropomyosin (magenta), and nuclei were identified by immunostaining for DsRed (green). Scale bar, 10 μm . (B, C) Distance between the dorsal end of the muscle and nearest nucleus (B) and between the ventral end of the muscle and nearest nucleus (C) for indicated genotypes. Each data point represents the average distance within a single embryo. Error bars indicate the SD from 20 embryos. Student's t test was used for comparison to controls. * $p < 0.05$, ** $p < 0.005$, *** $p < 0.0005$, **** $p < 0.00005$.

these data suggest that the activities of CNM- and EDMD-linked genes are temporally distinct.

To test whether the variation of phenotypes seen in the RNAi experiments was due to variation in RNAi efficiency, we tested embryos that were homozygous for either the *bocks*^{DP01391} or the *klar*¹ null allele (Welte et al., 1998). In *bocks*^{DP01391} and *klar*¹ embryos, nuclei were clustered near the ventral end of the muscle (Figure 3A), with nuclei positioned 53 and 43% farther from the dorsal ends of muscles in *bocks*^{DP01391} and *klar*¹ embryos, respectively (Figure 3B). In addition, compared with controls, nuclei were 25 and 18% closer to the ventral muscle ends in *bocks*^{DP01391} and *klar*¹ embryos, respectively (Figure 3C). The null allele for *Amph*, *Amph*²⁶ (Zelhof et al., 2001), did not affect the position of nuclei relative to the muscle ends (Figure 3, A–C).

There was an increase, however, in the appearance of individual nuclei near the center of the muscle in *Amph*²⁶ embryos. Furthermore, in a small number of *klar*¹ and *bocks*^{DP01391} embryos, a single nucleus appeared to be positioned near the dorsal end of the muscle. Therefore we further measured the distribution of nuclei within the muscle. First, we determined the distribution of nuclei by line-scan analysis of the *apRed* (nuclei) signal in the LT muscles in each genotype (Figure 4, A and B). In both *twist-GAL4*, *apRed* and

DMef-GAL4, *apRed* control embryos, there were two peaks—one near the dorsal end and one near the ventral end of the muscle (Figure 4, A, B, and G). Analysis of *klar*¹ embryos revealed three distinct phenotypes (Figure 4, A and G). In *klar*¹ embryos with a nucleus near the dorsal end of the muscle, there were distinct peaks, but the breadth of the peak near the ventral end was greater than the breadth of peak near the dorsal end, indicating that the ventral cluster is larger. In *klar*¹ embryos with a single cluster of nuclei, the intensity profile showed a single broad peak near the ventral end of the muscle. Finally, in embryos with a spread phenotype, the nuclei extend from the dorsal portion of the muscle to the ventral portion of the muscle without any discernible gaps, which would appear as troughs in the intensity profiles. Similar data were obtained by analysis of *bocks*^{DP01391} embryos. These data suggest that the distribution of nuclei between the dorsal and ventral clusters is disrupted by the loss of *klarsicht* or *bocksbeutel*.

To support these data, we measured the areas of the clusters of nuclei. The size of the dorsal cluster of nuclei was reduced in *bocks*^{DP01391} and *klar*¹ embryos compared with controls (Figure 4C). Conversely, the area of the ventral cluster of nuclei was increased in *bocks*^{DP01391} and *klar*¹ embryos compared with controls (Figure 4D). The total area of the muscle filled by the nuclei was equal in

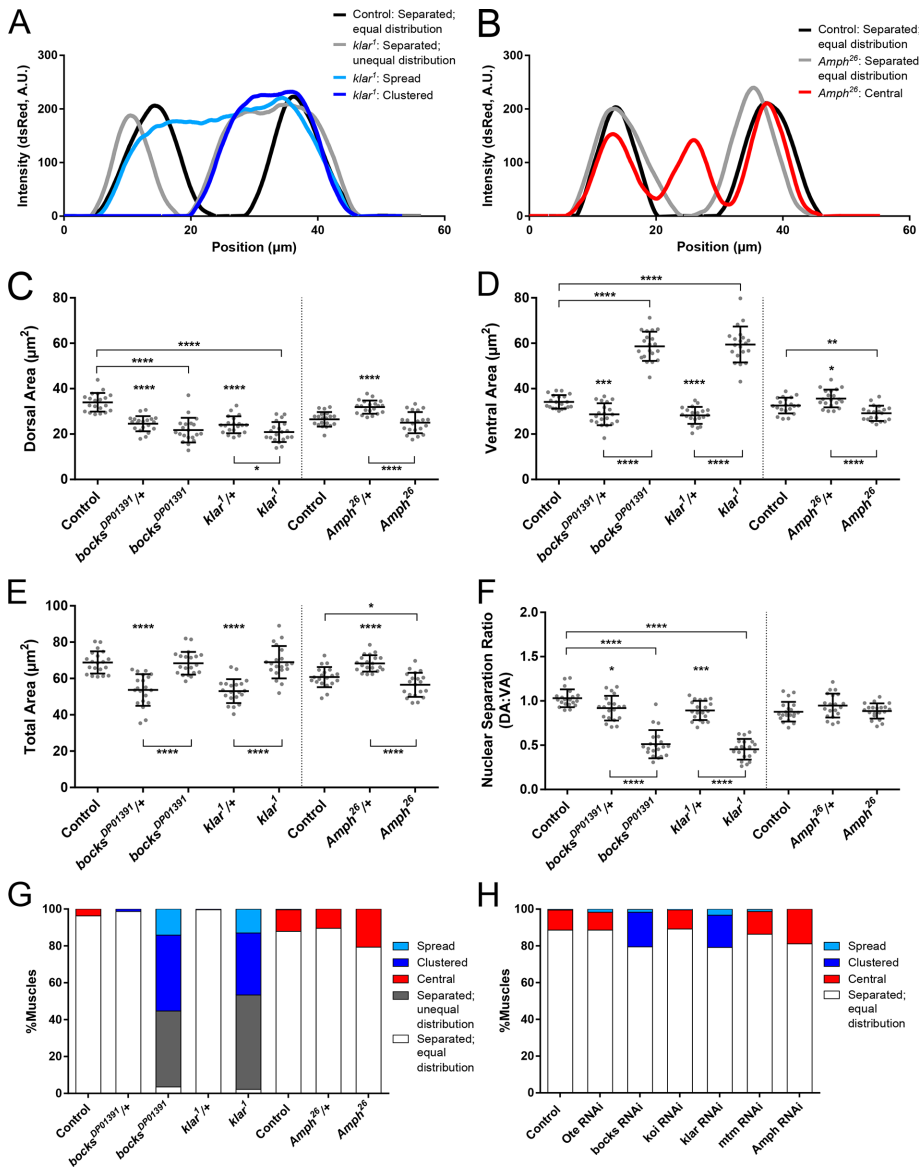


FIGURE 4: *Bocksbeutel*, *klarsicht*, and *Amphiphysin* are necessary for proper association of nuclear clusters in *Drosophila* embryos. (A, B) Averaged line scans of dsRed intensity for each nuclear phenotype observed in *klar¹* mutants (A) and *Amph²⁶* mutants (B) compared with controls. Each line represents the average of line scans measured from 10 LT muscles within 10 different embryos. Position correlates with the length of the muscle, starting at the dorsal end (position = 0 μm). (C–E) Area of nuclei located near the dorsal end of the muscle (C), area of nuclei located near the ventral end of the muscle (D), and total area of the muscle occupied by nuclei (E) for the indicated genotypes. (F) The relative distribution of nuclei between the dorsal half of the muscle and the ventral half of the muscle in each of the indicated genotypes. Each data point represents the average area within a single embryo. Error bars indicate SD from 20 embryos. Student's t test was used for comparison to controls. * $p < 0.05$, ** $p < 0.005$, *** $p < 0.0005$, **** $p < 0.00005$. (G) Frequency at which each phenotype was found in each of the indicated genotypes. (H) Frequency at which each phenotype was found when each of the indicated UAS-RNAi constructs was driven with *DMef2-GAL4*.

bocks^{DP01391}, *klar¹*, and control embryos (Figure 4E). The total area filled by nuclei, however, was reduced in both *bocks^{DP01391}* and *klar¹* heterozygotes compared with controls. The decrease in nuclear areas can be explained as a function of decreased muscle size. To maintain animals with the null mutations of *bocks^{DP01391}* and *klar¹*, each allele is carried over the *TM6b* balancer, which also carries the *Tb¹* dominant mutation (Lattao et al., 2011), resulting in short, wide muscles (Supplemental Figure S4A). To control for these differences

in muscle size across all genotypes, we determined the percentage of total muscle area that was occupied by all nuclei. In all genotypes tested, nuclei comprised ~25% of the total muscle area (Supplemental Figure S4B), and the sum of nuclear areas correlated with muscle size in all genotypes (Supplemental Figure S4, C–E).

Finally, the ratio of the size of the dorsal cluster of nuclei compared with the ventral cluster of nuclei was significantly reduced in *bocks^{DP01391}* and *klar¹* embryos compared with controls and heterozygotes (Figure 4F). In controls, the average ratio was ~1, whereas in *bocks^{DP01391}* and *klar¹* embryos, the cluster of nuclei near the ventral end of the muscle was on average twice as large as the cluster near the dorsal end. In total, these data suggest that *bocksbeutel* and *klarsicht* are required for the separation of nuclei and their distribution into two distinct clusters of equal size that then move to opposed ends of the muscle.

Similar analysis was completed on *Amph²⁶* embryos. *Amph²⁶* embryos had nuclei properly distributed between the dorsal and ventral ends, with only slight differences compared with controls (Figure 4, B and G). However, in 20% of muscles, there was an additional peak near the center of the cell, indicating that there was a mispositioned nucleus. This central nucleus was on average equidistant from both the dorsal cluster and the ventral cluster of nuclei (Figure 4B).

These data are supported by the measurements of cluster size. The dorsal cluster in *Amph²⁶* embryos is smaller, but insignificantly so, than with control embryos (Figure 4C). The ventral cluster in *Amph²⁶* embryos is smaller than with control embryos (Figure 4D). The total area occupied by nuclei is also slightly smaller in *Amph²⁶* embryos than with controls (Figure 4E). However the ratio of the size of the dorsal cluster compared with the ventral cluster of nuclei is equal in *Amph²⁶* embryos and control embryos (Figure 4F). These data suggest that separation of nuclei into distinct clusters of equal size is not affected by the loss of *Amphiphysin*. However, the presence of central nuclei suggests that clusters of nuclei are not properly maintained during migration toward the muscle end. Furthermore, that the ratio of the size of the dorsal cluster compared with the ventral cluster is not affected suggests that the nuclei that occupy the center of the muscle originate from dorsal and ventral clusters with equal frequency.

On the basis of these measurements, we counted the frequency of distinct phenotypes (Figure 4G). In controls, nuclei were properly separated into two distinct, dorsal and ventral groups of equal size in most embryos (96%, *twist-GAL4*, *apRed*; 90%, *DMef2-GAL4*, *apRed*). In *Amph²⁶* embryos, nuclei were separated into distinct

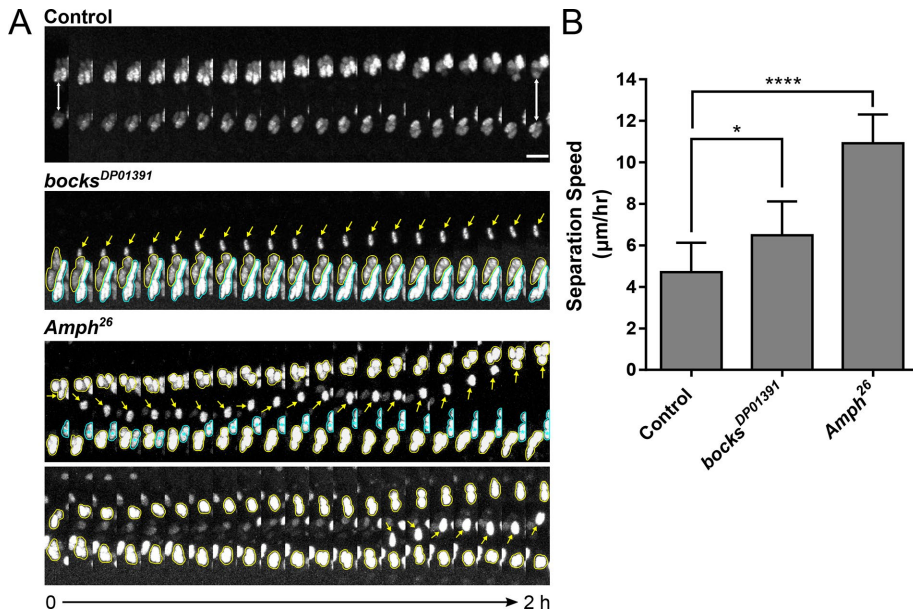


FIGURE 5: Both *bocksbeutel* and *Amphiphysin* regulate associations between myonuclei in *Drosophila* embryos. (A) Montages from time-lapse images showing the separation of the dorsal and ventral clusters of nuclei within a single LT muscle of late stage 15 embryos for the indicated genotypes. Embryos are oriented such that top is dorsal, bottom is ventral, left is anterior, and right is posterior. Yellow arrows indicate an escaper nucleus that separates from the ventral group (*bocks^{DP01391}*) or a nucleus that prematurely dissociates from its original cluster, indicated by yellow circles (*Amph²⁶*). Nuclei outlined in cyan indicate additional nuclei from the neighboring LT muscle. Scale bar, 10 μm. (B) Speed at which the dorsal and ventral clusters of nuclei separate for the indicated genotypes. Error bars indicate SD from 10 LT muscles. Student's t test was used for comparison to controls. * $p < 0.05$, **** $p < 0.00005$.

clusters, but centrally mispositioned nuclei were identified in 20% of muscles, compared with <10% of muscles in controls (Figure 4G). In contrast, central nuclei were not found in either *bocks^{DP01391}* or *klar¹* embryos. However, nuclei were clustered near the ventral end of 41 and 33% of the muscles in *bocks^{DP01391}* or *klar¹* embryos, respectively. In addition, in 14% *bocks^{DP01391}* embryos and in 13% of *klar¹* embryos, nuclei were spread through the center of the myofiber, with no distinct dorsal or ventral clusters (Figure 4G).

Similar analysis of embryos that had undergone muscle-specific RNAi-mediated depletion produced similar data. Central nuclei were found at an increased frequency in embryos that expressed RNAi under the control of *DMef2-GAL4* or *twist-GAL4* (Figure 4H and Supplemental Figure S2H). In addition, muscle-specific depletion of *klar* and *bocks* caused phenotypes that resembled the nulls. Specifically, in ~20% of embryos, the nuclei were in a single cluster near the ventral end of the muscle rather than in two clusters near either end of the muscle (Figure 4H and Supplemental Figure S2, E and H).

Together these data suggest that the EDMD-linked genes *klar-sicht* and *bocksbeutel* and the CNM-linked gene *Amphiphysin* are all necessary for nuclear movement during embryonic muscle development. In addition, the function of each factor with respect to nuclear position is muscle autonomous. However, the specific contributions of the EDMD-linked genes are distinct from the contributions of the CNM-linked gene. That nuclei are in a single cluster when *bocks* or *klar* is disrupted suggests that these factors are necessary to separate nuclei from one another. That nuclei are found in the center of the muscle when *Amph* is disrupted suggests that *Amph* is necessary to maintain the interactions between nuclei.

To test these hypotheses directly, we analyzed the movement of myonuclei during embryonic development. In control embryos, dorsal clusters of nuclei and ventral clusters of nuclei moved away from one another at a rate of ~5 μm/h (Figure 5, A and B) as previously described (Folker et al., 2014). During this movement, nuclei remained within their respective clusters and did not change direction (Figure 5A). In *bocks^{DP01391}* embryos, nuclei remained in a single cluster without splitting into separate clusters (Figure 5A). However, on the occasion that a single nucleus did escape from a cluster, it moved directly toward the dorsal end of the muscle at a rate of >6 μm/h (Figure 5B). This demonstrated that nuclei are in a single cluster because the cluster cannot be resolved and not because nuclei move back to their starting point. In addition, the fact that the rare nuclei that escape the cluster do move directionally to a proper position suggests that the machinery and directional cues for myonuclear movement are present.

Nuclear movement in *Amph²⁶* embryos was significantly different. The clusters of nuclei were only loosely associated as they moved toward the muscle end. Nuclei regularly dissociated from a cluster and moved into the middle of the muscle (Figure 5A). Furthermore, nuclei dissociated from both the dorsal and ventral cluster of nuclei and moved either back to their original cluster or to the other cluster without preference (Figure 5A). Finally, the clusters of nuclei moved significantly faster in *Amph²⁶* embryos than with either control or *bocks^{DP01391}* embryos. These data explain the relatively low abundance of centrally positioned nuclei in embryos (Figure 4, G and H). Because the nuclei occupy the center of the muscle transiently before moving to either the dorsal or ventral cluster, central nuclei were found only in a subset of muscles by fixed-embryo analysis. Together these data suggest that *bocksbeutel* is necessary for the separation of nuclei from one another, and *Amphiphysin* is necessary to maintain the association of nuclei with one another.

Genetic interactions between microtubule motors and EDMD- and CNM-linked genes in the *Drosophila* larva

To determine whether there are distinct genetic interactions between the EDMD-linked and CNM-linked genes and established pathways known to affect nuclear positioning, we tested genetic interactions between microtubule motors and *bocksbeutel* and *Amphiphysin* with respect to nuclear positioning in larvae (Figure 6). The average internuclear distance was 69% of maximal for *Dhc64C^{4-19/+}*, *bocks^{DP01391/+}* larvae, compared with 76 and 72% of maximal for *Dhc64C^{4-19/+}* and *bocks^{DP01391/+}* individual heterozygotes, respectively (Figure 6B). Similarly, the average internuclear distance was 68% of maximal for *Khc^{8/+}*; *bocks^{DP01331/+}* larvae, compared with 72% of maximal for both *Khc^{8/+}* and *bocks^{DP01391/+}* individual heterozygotes (Figure 6B). However, in *Dhc64C^{4-19/+}*, *bocks^{DP01391/+}* and *Khc^{8/+}*; *bocks^{DP01331/+}*, nuclei were properly positioned relative to the muscle edge (Figure 6C). Furthermore, in those regions of the muscle where nuclei do form two lines, the two lines are properly

spaced relative to one another (Figure 6D). Conversely, *Dhc64C⁴⁻¹⁹* and *Khc⁸* do not genetically interact with *Amph²⁶* to regulate the distribution of nuclei throughout the muscle (Figure 6, E–H). Together these data indicate that *bocksbeutel* regulates nuclear positioning in larvae through a microtubule motor–dependent mechanism, whereas *Amphiphysin* regulates nuclear positioning through a microtubule motor–independent mechanism.

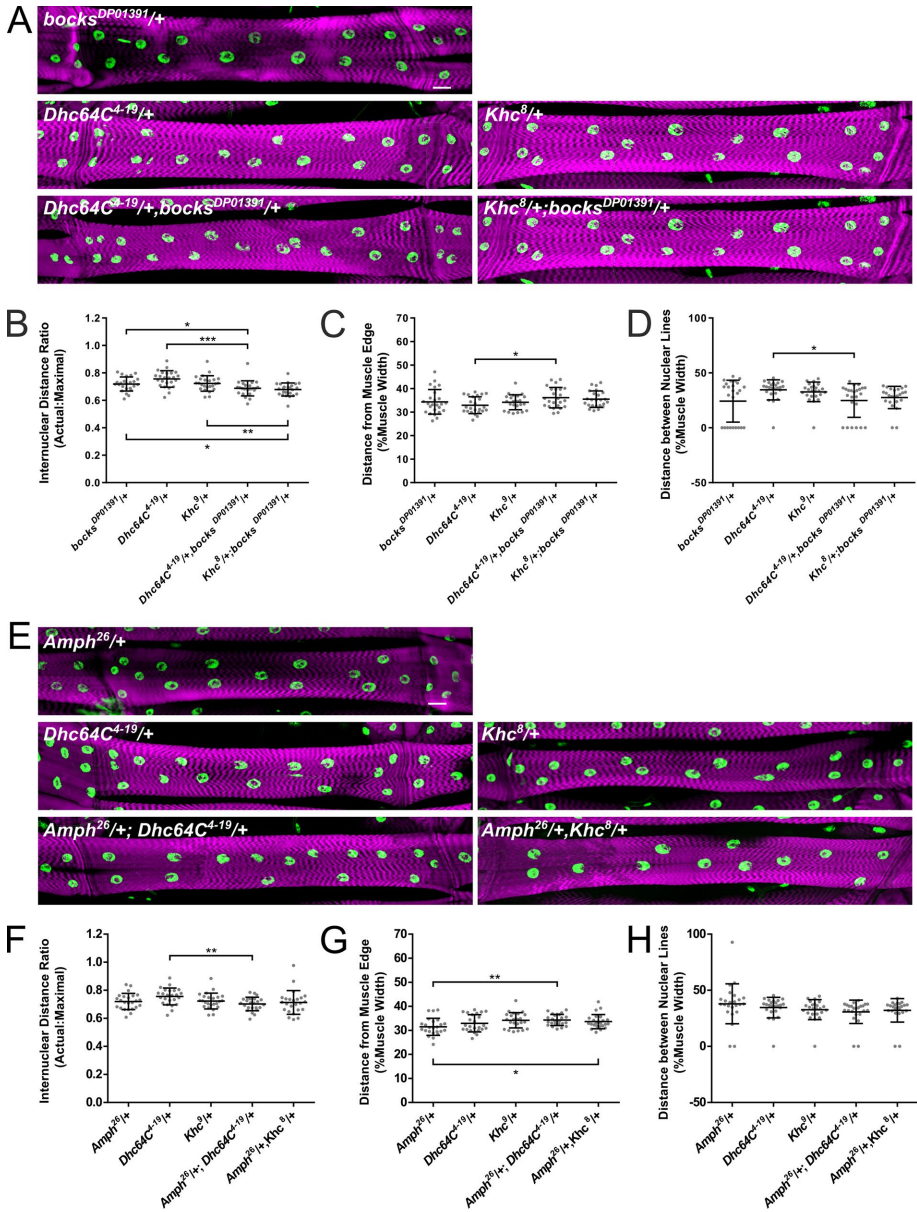


FIGURE 6: *Bocksbeutel* genetically interacts with *dynein* and *kinesin* to affect nuclear positioning within larval muscles. (A, E) Immunofluorescence images of VL3 muscles from stage L3 larvae of indicated genotypes. The sarcomeres were stained with phalloidin (magenta), and the nuclei were stained with Hoechst (green). Scale bar, 25 μ m. (B, F) The ratio of actual internuclear distance to maximal internuclear distance in larval muscles from the indicated genotypes. Data points indicate the average value for the internuclear distance ratio for all nuclei within a single VL3 muscle. (C, G) Distance between nuclei and the nearest muscle edge in larval muscles from the indicated genotypes. Data points indicate the average distance from the muscle edge of all nuclei within a single VL3 muscle. (D, H) Distance between nuclear lines in larval muscles from the indicated genotypes. Data points indicate the average distance between nuclear lines within a single VL3 muscle. Error bars indicate SD from 24 VL3 muscles. Student's t test was used for comparison to controls. * $p < 0.05$, ** $p < 0.005$, *** $p < 0.0005$.

Genetic interactions between *bocksbeutel* and the microtubule motor proteins dynein and kinesin in the *Drosophila* embryo

Next we investigated the genetic interactions between the microtubule motor proteins dynein and kinesin and the genes linked to EDMD and CNM. We completed double-heterozygote experiments to evaluate the genetic interactions between *bocks^{DP01391}* and both *Dhc64C⁴⁻¹⁹* and *Khc⁸*. The position of myonuclei in embryos that were *Dhc64C^{4-19/+};bocks^{DP01391/+}* double heterozygotes was different from that with each individual heterozygote (Figure 7, A–C). However, the phenotype was an intermediate of the individual heterozygotes. The distance between the muscle end and the nearest nucleus in *Dhc64C^{4-19/+};bocks^{DP01391/+}* double heterozygotes was increased compared with the same distance in *bocks^{DP01391/+}* embryos. However, compared with *Dhc64C^{4-19/+}* embryos, the distance between the muscle end and the nearest nucleus was decreased in *Dhc64C^{4-19/+};bocks^{DP01391/+}* double heterozygotes (Figure 7, B and C). These data suggest that *Dynein* and *bocksbeutel* do not interact to regulate myonuclear movement in embryos. However, there was a clear interaction between *bocks^{DP01391}* and *Khc⁸* with respect to the distribution of nuclei. With respect to the nuclear separation ratio, more nuclei were positioned within the ventral end of the muscles in the *Khc^{8/+};bocks^{DP01391/+}* embryos than in *bocks^{DP01391/+}* and *Khc^{8/+}* embryos (Figure 7D). In addition, qualitative analysis of the phenotypes also indicated an interaction between *bocks^{DP01391}* and *Khc⁸* (Figure 7E). The frequency of central nuclei in the *Khc^{8/+};bocks^{DP01391/+}* double heterozygote is increased compared with either single heterozygote. Similarly, we completed double-heterozygote experiments to evaluate the genetic interactions between *Amph²⁶* and both *Dhc64C⁴⁻¹⁹* and *Khc⁸* (Figure 7F). No genetic interaction was observed with either motor protein with respect to myonuclear position, nuclear distribution, or phenotypes (Figure 7, G–J). Together these data indicate that *bocksbeutel* regulates nuclear positioning in embryos through a microtubule motor–dependent mechanism, whereas *Amphiphysin* regulates nuclear positioning through a microtubule motor–independent mechanism.

Disruption of EDMD- and CNM-linked genes affects microtubule organization in the *Drosophila* larva

Because the nuclear membrane is one of the sites of the microtubule-organizing center in muscle (Tassin *et al.*, 1985; Zaal *et al.*, 2011; Espigat-Georger *et al.*, 2016), we investigated whether the depletion of *bocksbeutel* or *Amphiphysin* alters the organization of

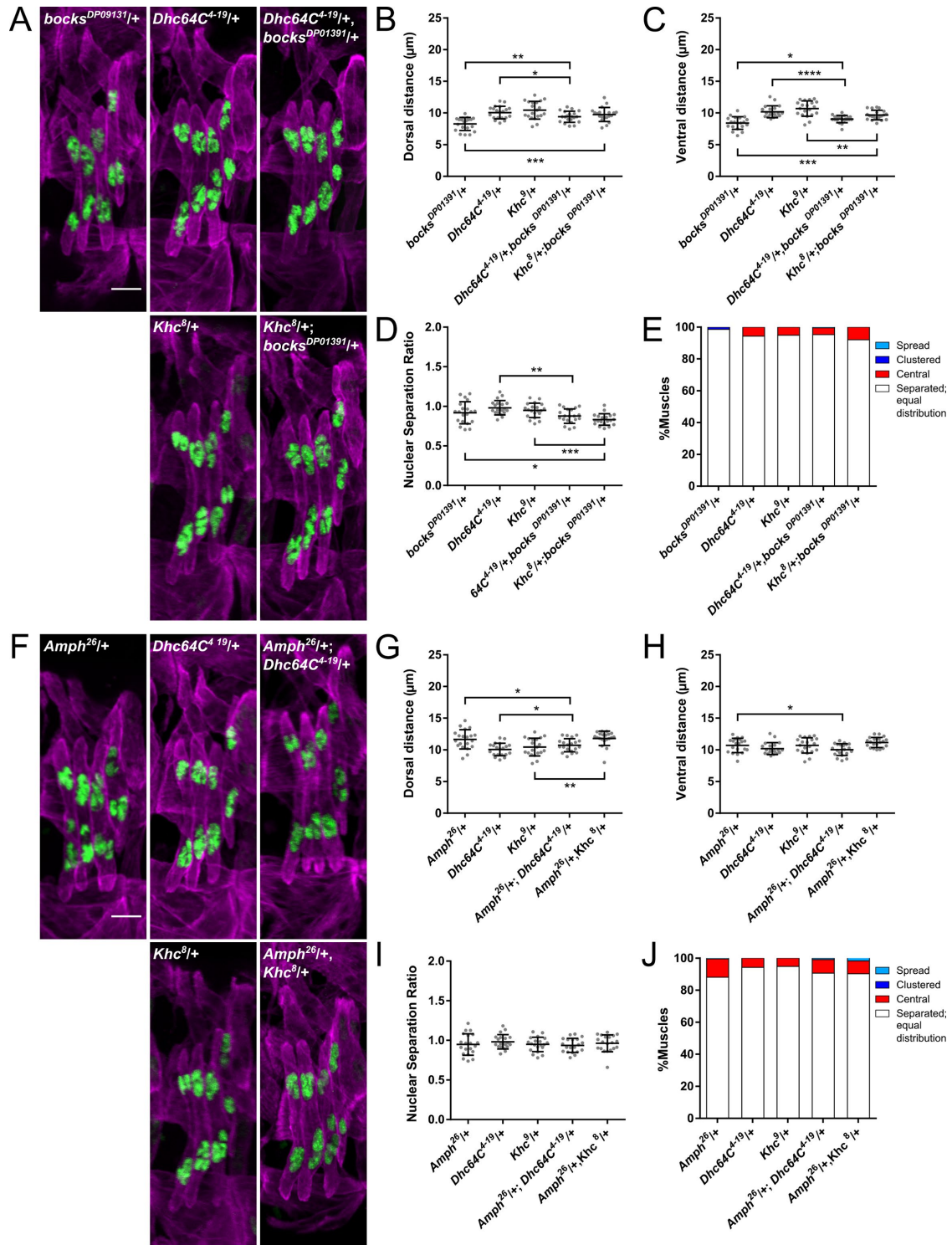


FIGURE 7: *Bocksbeutel* genetically interacts with dynein and kinesin to affect nuclear positioning within embryonic muscles. (A, F) Immunofluorescence images of the LT muscles in one hemisegment from stage 16 (16 h AEL) embryos. Embryos are oriented such that top is dorsal, bottom is ventral, left is anterior, and right is posterior. Muscles were identified by immunostaining for tropomyosin (magenta), and the nuclei were identified by immunostaining for DsRed (green) Scale bars, 10 μm. (B, C, G, H) Histograms indicating the distance between the dorsal end of the muscle and the nearest nucleus (B, G) and between the ventral end of the muscle and the nearest nucleus (C, H) in the indicated genotypes. (D, I) Nuclear distribution ratio between dorsal and ventral clusters of nuclei in indicated genotypes. (E, J) Qualitative analysis of nuclear phenotypes for indicated genotypes. For B–D and G–I, each data point indicates the average distance within a single embryo. Error bars indicate SD from 20 embryos. Student’s t test was used for comparison to controls. **p* < 0.05, ***p* < 0.005, ****p* < 0.0005, *****p* < 0.00005.

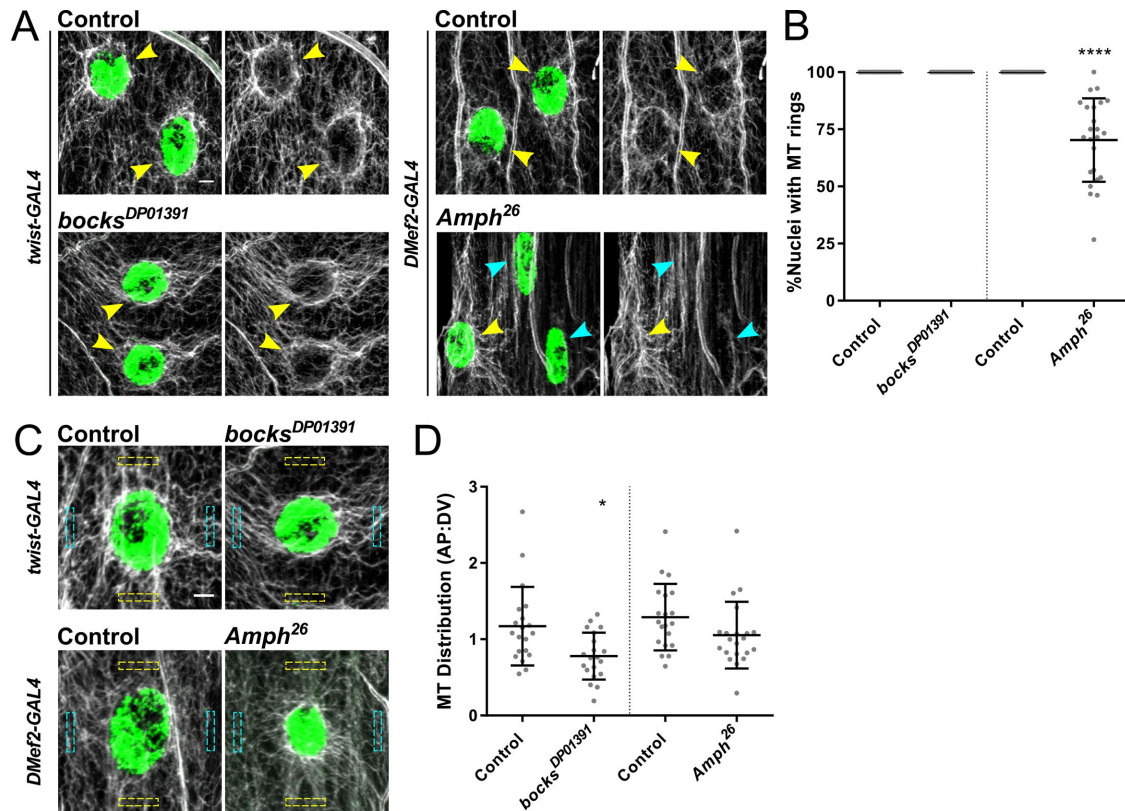


FIGURE 8: Both *bocksbeutel* and *Amphiphysin* are necessary for proper microtubule organization. (A) Immunofluorescence images of nuclei from VL3 muscles from stage L3 larvae. Microtubules were identified by immunostaining for α -tubulin (gray), and the nuclei were stained with Hoechst (green). Yellow arrowheads indicate nuclei with associated microtubule rings. Cyan arrowheads indicate nuclei lacking associated microtubule rings. Scale bar, 5 μ m. (B) Counts of nuclei with associated microtubule rings. Data points indicate percentage of nuclei within a single VL3 muscle of an L3 larva that have an associated microtubule ring. Student's t test was used for comparison to controls. (C) Immunofluorescence images of nuclei from VL3 muscles from stage L3 larvae. Microtubules were identified by immunostaining for α -tubulin (gray), and the nuclei were stained with Hoechst (green). Yellow boxes indicate location of anterior and posterior measurements for microtubule integrated intensity. Cyan boxes indicate location of dorsal and ventral measurements of microtubule integrated intensity. Scale bar, 5 μ m. (D) The polarity of microtubules around the nucleus in larval muscles. Data points indicate the ratio of the average integrated density from the anterior and posterior positions to the average integrated density of microtubule staining around the dorsal and ventral positions of a single nucleus. * $p < 0.05$, **** $p < 0.00005$. *Bocksbeutel* genetically interacts with *dynein* and *kinesin* to affect nuclear positioning within embryonic muscles.

the microtubule cytoskeleton. The microtubule network appeared normal in embryos, but the small cell size and the clustering of nuclei prohibited careful analysis. Therefore we evaluated microtubule organization in larvae (Figure 8, A and C). First, we investigated whether nuclei were able to nucleate microtubules by counting the number of nuclei that had a ring of microtubule staining around them (Figure 8A). In control and *bocks*^{DP01391} larvae, 100% of nuclei had a ring of microtubules, whereas in *Amph*²⁶ larvae, only 69% of nuclei had associated microtubule rings (Figure 8B). We also measured microtubule distribution around nuclei with microtubule rings (Figure 8, C and D). We measured the distribution of microtubules as the ratio of intensity of tubulin staining oriented dorsally and ventrally from the nucleus versus the intensity of tubulin staining oriented anteriorly and posteriorly from the nucleus. In *bocks*^{DP01391} larvae, the distribution of microtubules around the nucleus was altered, with more microtubules emanating in the dorsal/ventral direction than in the anterior/posterior direction, as demonstrated by the microtubule distribution ratio of 0.77 compared with 1.17 in controls (Figure 8D).

The microtubules were evenly distributed around nuclei with associated microtubule rings in *Amph*²⁶ larvae, with a distribution ratio of 1.04 (Figure 8B). These data indicate that both *bocksbeutel* and *Amphiphysin* are necessary for proper microtubule organization in larvae but that *bocksbeutel* and *Amphiphysin* affect different aspects of microtubule organization.

DISCUSSION

We used *Drosophila* musculature to investigate whether aberrant nuclear position that is related to EDMD and CNM results from a common mechanism. We find that disruption of EDMD- and CNM-linked genes in *Drosophila* recapitulates the phenotypes of mispositioned nuclei evident in the human diseases (Table 1). Furthermore, the effects on nuclear position are evident in both the embryo and the larvae, and the mechanism by which nuclear position is disrupted is muscle autonomous. However, these data also indicate that the specific phenotype is different, depending on whether EDMD- or CNM-linked genes are disrupted.

Genotype	Embryo				Larva			
	Dorsal	Ventral	Central	Clustered	Distribution	Edge	Between lines	Locomotion
<i>bocks</i> ^{DP01391/+}	-	-	-	-	-	-	-	-
<i>bocks</i> ^{DP01391}	+	+	-	+	+	+	+	+
<i>klar</i> ^{1/+}	-	-	-	-	-	-	-	-
<i>klar</i> ¹	+	+	-	+	+	+	+	+
<i>Amph</i> ^{26/+}	-	-	-	-	-	-	-	-
<i>Amph</i> ²⁶	-	-	+	-	+	-	-	+
<i>Ote</i> RNAi	+	-	-	-	+	+	-	n.a.
<i>bocks</i> RNAi	+	+	-	+	+	+	-	n.a.
<i>koi</i> RNAi	+	-	-	-	+	+	+	n.a.
<i>klar</i> RNAi	+	+	-	+	+	+	+	n.a.
<i>mtm</i> RNAi	+	-	-	-	+	-	+	n.a.
<i>Amph</i> RNAi	-	+	+	-	+	+	-	n.a.

TABLE 1: Summary of nuclear positioning defects in the tested genotypes.

In interpreting these data, it is important to note that each of the alleles used is a null. However, only the *emerin* mutation leading to EDMD is believed to be a complete loss of function. The *Amph* mutations that have been linked to CNM, and the *SYNE1* and *SYNE2* mutations that have been linked to EDMD are missense mutations. The effect of these specific mutations that cause disease is a critical next step. Nevertheless, that the functions of these genes with respect to nuclear position are disrupted by null mutations indicates that these are functions to explore in disease models.

In embryos with disrupted expression of *Amph* (CNM-linked gene), there is an increase in the frequency of nuclei that populate the center of the muscle. The increased number of central nuclei suggests that the clusters of nuclei are not tightly maintained as they move toward the ends of the muscles. More directly, nucleus–nucleus interactions may be inhibited. Conversely, *bocks* and *klar*—nuclear envelope proteins related to EDMD-linked genes—are necessary for the dissociation of nuclei from one another. This suggests that nucleus–nucleus interactions are too tightly maintained. Together these data suggest that the two sets of genes have opposing functions with respect to nucleus–nucleus interactions and nuclear movement. These conclusions are supported by live-embryo time-lapse microscopy, which clearly demonstrated that most nuclei are stuck within a single cluster in *bocks*^{DP01391} embryos, whereas nuclei dissociate from clusters at a high frequency in *Amph*²⁶ embryos. In addition, the speeds at which the clusters of nuclei separate from each other is increased in *bocks*^{DP01391} embryos and increased to a greater degree in *Amph*²⁶ embryos. This suggests that the interactions between nuclei restrict nuclear movement. Therefore, when such interactions are inhibited in *Amph*²⁶ embryos, nuclei can move more freely in terms of both direction and speed. This is complicated by the observation that nuclei move faster in *bocks*^{DP01391} embryos than in controls. One explanation for this is that the nucleus that escapes and moves dorsally has limited interactions with other nuclei and therefore is free to move more quickly.

It is important to note that the interactions between nuclei are likely indirect. The proteins encoded for by *klarsicht* and *bocksbeutel* are nesprin and emerlin proteins, respectively. Each of these proteins can localize to the outer nuclear envelope and regulate

interactions between the nucleus and the cytoskeleton (Starr and Han, 2002; Salpingidou et al., 2007; Chang et al., 2013). In addition, in muscle, the nuclear envelope is crucial for the organization of the microtubule cytoskeleton (Tassin et al., 1985; Espigat-Georger et al., 2016). Therefore it is likely that nucleus–nucleus interactions are mediated by the cytoskeleton. Consistent with this, loss of either *bocks* or *Amph* disrupts microtubule organization (Figure 8). In *bocks*^{DP01391} larvae, the distribution of microtubules around each nucleus was polarized along the dorsal/ventral axis of the muscle compared with control larvae, in which the microtubules were evenly distributed around the each nucleus. In *Amph*²⁶ larvae, when microtubules emanate from each nucleus, they are distributed evenly, as in controls. However, not all nuclei have associated microtubules. Together these data suggests a role for the microtubule cytoskeleton in mediating the balance between nucleus–nucleus interactions.

The distinction in phenotype that is caused by disruptions in EDMD-linked genes versus disruptions in CNM-linked genes is maintained in the larval stage of *Drosophila* development. The inability to resolve the single chain of nuclei in the larvae with disrupted EDMD-linked genes is directly comparable to the single cluster of nuclei found in embryos and further suggests that EDMD-linked genes are necessary to resolve nucleus–nucleus interactions. Similarly, the few mispositioned nuclei in larvae with disrupted CNM-linked genes are consistent with nuclei being disengaged from other nuclei and therefore occupying a space too near another nucleus.

RNAi experiments were used to demonstrate that the effects of these genes on nuclear position in muscle were muscle autonomous and suggested that some functions are temporally restricted. With respect to each RNAi, continued depletion of the protein by expression of the RNAi under the control of the *DMef2-Gal4* driver did not exaggerate the general evenness of nuclear distribution compared with the more acute depletion driven by *twist-Gal4* (compare Figure 2 to Supplemental Figure S2). In fact, with regard to one factor, *mtm*, the phenotype was less dramatic, suggesting that it primarily functions early in development. Furthermore, the position of nuclei relative to the edge of the muscle was significantly affected only when specific proteins were depleted throughout muscle development

with the *DMef2-Gal4* driver. The importance of nuclear position relative to the muscle edge is not clear. However, these data suggest that each of these genes contributes to nuclear position by several mechanisms that may be separated by developmental time.

Despite the general disruption of nuclear positioning across all genotypes analyzed, there were some notable differences in the severity of phenotypes produced between proteins associated with EDMD. Although both are considered *Drosophila* homologues of emerin, depletion of *bocksbeutel* more strongly disrupted nuclear positioning than depletion of *Otefin*. These differences may suggest that *bocksbeutel* and *Otefin* may have distinct functions and regulatory roles in the process of nuclear positioning. This would not be the first indication that *bocksbeutel* and *Otefin*, the two *Drosophila* homologues of emerin, have distinct functions. With respect to fertility, *Drosophila* are more sensitive to the loss of *Otefin* than they are to the loss of *bocksbeutel* (Barton et al., 2014). Because we find the opposite effect with respect to nuclear position in muscle, these data together suggest that *bocksbeutel* and *Otefin* may have specific roles in different tissues.

Our conclusion that EDMD- and CNM-linked genes disrupt nuclear position by distinct mechanisms is further supported by the differences in their genetic interactions. Whereas *bocks* genetically interacts with the microtubule motors dynein and kinesin, *Amph* does not. These data suggest that *bocks* regulates nuclear movement via the described microtubule-dependent pathways (Folker et al., 2012, 2014; Metzger et al., 2012). The mechanism by which *Amph* regulates nuclear movement and nucleus–nucleus interactions is not clear. Recent data from cell culture suggest that this may be an actin-dependent process (Falcone et al., 2014; D'Alessandro et al., 2015). However, we have shown that *Amph* is necessary for proper microtubule organization at the nucleus, suggesting that nucleus–nucleus interactions may be microtubule dependent.

In all, these data suggest that although mispositioned nuclei are a phenotype common to CNM and EDMD, the underlying mechanism is different in each disease. That genes linked to distinct muscle diseases affect nuclear position by different mechanisms is critical to understanding the effect of nuclear position on muscle health. These conclusions dictate that the mechanisms that underlie mispositioned nuclei in each muscle disease must be individually identified and not considered collectively. However, these data also suggest that there may be a web of genetic pathways that have counteracting and balancing effects. Thus there may be viable methods to improve nuclear distribution either genetically or pharmacologically.

MATERIALS AND METHODS

Drosophila genetics

All stocks were grown under standard conditions at 25°C. Stocks used were *apRed* (Richardson et al., 2007), *bocks*^{DP01391} (21846; Bloomington *Drosophila* Stock Center), *klar*¹ (3256; Bloomington *Drosophila* Stock Center), *Amph*²⁶ (6498; Bloomington *Drosophila* Stock Center), UAS-*bocks* RNAi (38349; Bloomington *Drosophila* Stock Center), UAS-*klar* RNAi (36721; Bloomington *Drosophila* Stock Center), UAS-*koi* RNAi (40924; Bloomington *Drosophila* Stock Center), UAS-*Ote* RNAi (39009; Bloomington *Drosophila* Stock Center), UAS-*mtm* RNAi (31552; Bloomington *Drosophila* Stock Center), UAS-*Amph* RNAi (53971; Bloomington *Drosophila* Stock Center), *Dhc64C*⁴⁻¹⁹ (Gepner et al., 1996), and *Khc*⁸ (Brendza et al., 1999). Mutants were balanced and identified using *CyO*, *DGY* and *TM6b*, *DGY*. UAS-RNAi constructs were driven specifically in the mesoderm using *twist-GAL4*, *apRed*, specifically in the muscle using *DMef2-*

GAL4, *apRed*, or specifically in larval muscles using *MHC-GAL4*. Regarding *apRed* specifically, this fly expresses a nuclear localization signal fused to the fluorescent protein DsRed downstream of the *apterous* mesodermal enhancer. This results in the specific labeling of the nuclei within the lateral transverse muscles of the *Drosophila* embryo (Richardson et al., 2007). The *twist-GAL4*, *apRed*, *DMef2-GAL4*, *apRed* *Drosophila* lines were made by recombining the *apRed* promoter and the specific *GAL4* driver. In the case of *twist-GAL4*, *apRed*, both elements are on the second chromosome. In the case of *DMef2-GAL4*, *apRed*, both elements are on the third chromosome. There are slight variations between the two genotypes, so each was used as a control in all experiments.

Larval locomotion

Larval speed was measured as previously described (Louis et al., 2007; Metzger et al., 2012) with minor modifications. Stage 16 and 17 embryos were selected for the presence or absence of fluorescent balancers and placed on yeast-coated molasses agar plates at 21°C overnight. L1 larvae were selected and placed into a vial containing standard fly food. After 4 d, L3 larvae were picked from the vial and tracked on a 3% agarose gel as they crawled toward an odor source of ethyl butyrate (32.5%; 15701; Sigma-Aldrich) diluted in paraffin oil (18512; Sigma-Aldrich). Larvae were tracked with an iPhone (Apple) using OSnap! Pro (Justin Cegnar) for 3 min, with images taken every 5 s. Tracks were processed using the Manual Tracking plug-in on ImageJ software (National Institutes of Health). At least 20 larvae were tracked for each genotype.

Immunohistochemistry

Embryos were collected at 25°C and washed in 50% bleach to remove the outer membrane, washed with water, and then fixed in 50% Formalin (HT501128; Sigma-Aldrich) diluted in 1:1 heptane for 20 min to allow permeabilization. In all cases, embryos were devitelinated by vortexing in a 1:1 methanol:heptane solution.

Larvae were dissected as previously described (Louis et al., 2007; Metzger et al., 2012) with minor modifications. Larvae were dissected in ice-cold 1,4-piperazinediethanesulfonic acid (PIPES) dissection buffer containing 100 mM PIPES (P6757; Sigma-Aldrich), 115 mM D-sucrose (BP220-1; Fisher Scientific), 5 mM trehalose (182550250; Acros Organics), 10 mM sodium bicarbonate (BP328-500; Fisher Scientific), 75 mM potassium chloride (P333-500; Fisher Scientific), 4 mM magnesium chloride (M1028; Sigma-Aldrich), and 1 mM ethylene glycol tetraacetic acid (28-071-G; Fisher Scientific) and then fixed with 10% Formalin (HT501128; Sigma-Aldrich).

Antibodies for embryo staining were used at the following final dilutions: rabbit anti-dsRed, 1:400 (632496; Clontech); rat anti-tropomyosin, 1:200 (ab50567; Abcam), and mouse anti-green fluorescent protein, 1:50 (GFP-G1; Developmental Studies Hybridoma Bank). Mouse anti- α -tubulin (1:200, T6199; Sigma-Aldrich) was used in larvae. Conjugated fluorescent secondary antibodies used were Alexa Fluor 555 donkey anti-rabbit (1:200), Alexa Fluor 488 donkey anti-rat (1:200), and Alexa Fluor 647 donkey anti-mouse (1:200; all Life Technologies). Alexa Fluor 488 donkey anti-mouse (1:200; Life Technologies), Acti-stain 555 phalloidin (1:400; PHDH1-A; Cytoskeleton), and Hoechst 33342 (1 μ g/ml) were used in larvae. Embryos and larvae were mounted in ProLong Gold (P36930; Life Technologies) and imaged with an Apochromat 40 \times /1.4 numerical aperture (NA) objective with a 1.0 \times optical zoom for all embryo images on a Zeiss 700 LSM. Larvae were imaged using the same microscope and objective lens at 0.5 \times optical

zoom for nuclear positioning analysis and 2.0× optical zoom for microtubule analysis.

Analysis of nuclear position in larvae

We developed a means to measure internuclear distance that takes into account nuclear count and muscle size in order to determine how evenly nuclei are positioned, as opposed to how close together nuclei are. This measurement represents how ideally nuclei are positioned (Figure 4). In this method, the actual internuclear distance is determined by measuring the distance from the center of each nucleus to the center of its nearest nuclear neighbor (Figure 4A). The nearest nucleus could be in any direction relative to the nucleus in question. Thus sometimes the nearest nucleus was positioned adjacently on the long axis of the muscle, whereas the nearest neighbor for another nucleus might be adjacent on the short axis of the muscle. Next the area of the muscle was measured and the number of nuclei counted (Figure 4B). The maximal internuclear distance was determined by taking the square root of the muscle area divided by the nuclear count (Figure 4C). This value represents the distance between nuclei if internuclear distance was fully maximized. The ratio between the actual internuclear distance and the maximal internuclear distance ratio was then used to determine how even nuclei were distributed. This allows us to essentially normalize the internuclear distance to both nuclear count and muscle area, which leads to a more representative means of comparison between muscles, larvae, and genotypes.

In addition, the distance of each nucleus from the lengthwise edge of the muscle was determined by measuring the shortest distance from the center of the nucleus to the nearest long edge of the muscle. Similarly, the distance between the parallel lines of nuclei in each muscle was measured. To be considered a line of nuclei, it was necessary for at least four nuclei that covered at least 25% of the muscle length to be included. Nuclei were considered to be in the same nuclear line if the nuclei were present in the same dorsal or ventral half of the muscle. The distance between nuclear lines was measured by using the segmented line tool on ImageJ software to trace the nuclear lines; then the average distance between each line was determined. When only one nuclear line was present, the distance between nuclear lines was considered to be zero.

Analysis of nuclear position in embryos

Embryos were imaged at stage 16 based on overall embryo shape, the intensity of the apRed and tropomyosin signals, gut morphology, and the morphology of the trachea as previously described (Folker *et al.*, 2012). Images were processed as maximum intensity projections of confocal z-stacks, and measurements were acquired using the line function of ImageJ software. Dorsal and ventral end distances were taken from each LT muscle by measuring the distance between the closest group of nuclei to the dorsal or ventral muscle pole, respectively. All four LT muscles were measured in four hemisegments from each embryo. A total of 20 embryos were measured for each genotype taken from independent experiments. Statistical analysis was performed with Prism 4.0 (GraphPad). Student's *t* test was used to assess the statistical significance of differences in measurements between experimental genotypes to controls.

For qualitative nuclear phenotype analysis, embryos were scored on how nuclei positioned themselves within the first three LT muscles of each hemisegment. LT 4 was excluded for this analysis due to its variable muscle morphology. Nuclei were categorized as separated, equal distribution (nuclei properly segregated into two distinct, even clusters with a dorsal/ventral cluster size ratio ≥ 0.85 and ≤ 1.15 ; separated, unequal distribution (nuclei that segregated into

two disproportionate clusters); central (a nucleus or a small cluster of nuclei located in the middle of the myofiber that is not associated with either the dorsal or ventral group); clustered (nuclei remained in a single cluster toward the ventral end of the myofiber); or spread (nuclei are distributed through the myofiber with no distinct dorsal or ventral clusters). Line scans of dsRed intensity were performed on 10 LT muscles for each nuclear phenotype and averaged to determine the typical distribution of nuclei in each genotype.

Analysis of nuclear cluster area in embryos

Dorsal and ventral areas were taken from each (LT muscle by measuring the area of each cluster of nuclei near the dorsal or ventral muscle pole, respectively. All four LT muscles were measured in four hemisegments from each embryo using ImageJ. A total of 20 embryos were measured for each genotype taken from independent experiments. Total area of nuclear clusters in each LT muscle was calculated by adding the dorsal and ventral areas. The nuclear distribution ratio was calculated by dividing the dorsal area by the ventral area. Statistical analysis was performed with Prism 4.0. Student's *t* test was used to assess the statistical significance of differences in measurements between experimental genotypes and controls.

Live-embryo imaging

Embryos were collected at 25°C and washed in 50% bleach to remove the outer membrane, washed with water, and mounted with halocarbon oil (H8898; Sigma-Aldrich). Stage 15 embryos were selected for imaging based on gut morphology, the position of nuclei, and the intensity of the apRed signal, as previously described (Folker *et al.*, 2012). Time-lapse images were taken at an acquisition rate of 2 min/stack for 2 h with an Apochromat 40×/1.4 NA objective with 1.0× optical zoom on a Zeiss 700 LSM.

Movies were processed as maximum intensity projections of confocal z-stacks, and measurements were acquired using the line function in ImageJ. The separation speed of nuclei was taken by measuring the distance between dorsal and ventral nuclear clusters at time 0 and again at time 2 h. Statistical analysis was performed with Prism 4.0. Student's *t* test was used to assess the statistical significance of differences in measurements between experimental genotypes to controls.

Analysis of microtubule organization in larvae

The nuclei within a muscle that had microtubules nucleating from them were counted in VL3 muscles from L3 larvae. Nuclei were counted as nucleating microtubules if a ring of microtubules around the nucleus was present. A nuclear ring was classified as an increase in α -tubulin staining around the periphery of the nucleus and microtubules radiating from the nucleus. The percentage of nuclei with nuclear rings relative to all nuclei within the muscle was recorded.

Microtubule distribution around the nucleus was measured from VL3 muscles from L3 larvae by measuring the integrated density of the α -tubulin staining. The integrated density was measured from a 10 μm \times 2 μm region positioned 15 μm anteriorly and 15 μm posteriorly from the center of the nucleus. Similarly, the integrated density was also measured from a 2 μm \times 10 μm region positioned 15 μm dorsally and 15 μm ventrally from the center of the nucleus. Integrated densities from the anterior and posterior positions were averaged, as were the integrated densities from the dorsal and ventral positions. A ratio between the average anterior/posterior and dorsal/ventral integrated densities was used to determine the microtubule distribution ratio, with a value of 1 correlating with an

even distribution of microtubules around the nucleus, a value of >1 correlating with more microtubules distributed in the anterior/posterior regions relative to the nucleus, and a value of <1 correlating with more microtubules distributed in the dorsal/ventral regions relative to the nucleus.

RNA isolation, construction of cDNA library, and reverse transcription PCR

RNAi knockdown efficiency was measured in single embryos. Because muscle composes a small portion of the total mass of the embryo, RNAi was expressed ubiquitously to test efficiency using the *Tubulin-GAL4* driver. Embryos were washed in 50% bleach to remove the outer membrane and then washed with water. Single embryos of each genotype (*Tubulin-GAL4*, *UAS-Ote* RNAi, *UAS-bocks* RNAi, *UAS-koi* RNAi, *UAS-klar* RNAi, *UAS-mtm* RNAi, *UAS-Amph* RNAi) were selected at stage 17 of embryo development using the morphology of the gut and appearance of the trachea as previously described (Beckett and Baylies, 2007). To extract and isolate RNA, individual embryos were then crushed in an Eppendorf tube in 1 ml of TRIzol according to manufacturer's instructions (15596026; Invitrogen). RNA integrity and concentration were determined using the NanoDrop2000 system (Thermo Fisher Scientific). The cDNA library was established by performing reverse transcription using the SuperScript VILO cDNA Synthesis Kit (11-754-050; Invitrogen), according to manufacturer's protocol. Purified RNA was incubated with SuperScript III reverse transcriptase at 42°C for 2 h, and then reactions were terminated at 85°C for 5 min. RT-PCR was set up after inactivation of reverse transcription using the GoTaq Flexi DNA Polymerase (M8291; Promega). Primers were designed to amplify a ~120–base pair sequence within each targeted mRNA and a 315–base pair sequence within RP49 as a control. The denaturing temperature was 95°C, the annealing temperature was 49°C, the extension temperature was 72°C, and 40 amplification cycles were run. The primers used were *RP49* forward, 5'-TACAGGCCAA-GATCGTGAA-3'; *RP49* reverse, 5'-GACAATCTCCTTGCCTTCT-3'; *Ote* forward, 5'-AGCCCAAGGCTATGTGACTG-3'; *Ote* reverse, 5'-GATTCTGGCAAATGTGCTT-3'; *bocks* forward, 5'-TTACACAC-GCGAAGTTGACC-3'; *bocks* reverse, 5'-GTGGCTCGTATGTGGG-AAGT-3'; *koi* forward, 5'-CTCAGAACTGTCCCCTCACC-3'; *koi* reverse, 5'-GTGGCTCGTATGTGGGAAGT-3'; *klar* forward, 5'-CCC-TCCATATCAACCAGGAC-3'; *klar* reverse, 5'-GGCAAGACTTTC-GTCGAACT-3'; *mtm* forward, 5'-CAAAGTGGCAGACGGCTATT-3'; *mtm* reverse, 5'-GAACTACGACGGAGGTGCTC-3'; *Amph* forward, 5'-GGAAGGCAAAGTGCATCTC-3'; and *Amph* reverse, 5'-GAA-CAGATTTGGCCAGCATT-3'. PCR products were run on a 2% agarose gel and visualized with ethidium bromide. Gels were imaged using Typhoon FLA 9500 (GE Healthcare Life Sciences). Band intensities were quantified using ImageQuant. Values are normalized to expression of RP49 and displayed with control expression normalized to 1.

ACKNOWLEDGMENTS

Stocks obtained from the Bloomington *Drosophila* Stock Center (NIH P40OD018537) were used in this study. This work was supported by grants from the Hood Foundation and the American Heart Association to E.S.F.

REFERENCES

Auld AL, Folker ES (2016). Nucleus-dependent sarcomere assembly is mediated by the LINC complex. *Mol Biol Cell* 27, 2351–2359.
Barton LJ, Wilmington SR, Martin MJ, Skopec HM, Lovander KE, Pinto BS, Geyer PK (2014). Unique and shared functions of nuclear lamina LEM domain proteins in *Drosophila*. *Genetics* 197, 653–665.

Beckett K, Baylies MK (2007). 3D analysis of founder cell and fusion competent myoblast arrangements outlines a new model of myoblast fusion. *Dev Biol* 309, 113–125.
Brendza KM, Rose DJ, Gilbert SP, Saxton WM (1999). Lethal kinesin mutations reveal amino acids important for ATPase activation and structural coupling. *J Biol Chem* 274, 31506–31514.
Bruusgaard JC (2006). Distribution of myonuclei and microtubules in live muscle fibers of young, middle-aged, and old mice. *J Appl Physiol* 100, 2024–2030.
Bruusgaard JC, Liestøl K, Ekmark M, Kollstad K, Gundersen K (2004). Number and spatial distribution of nuclei in the muscle fibres of normal mice studied in vivo. *J Physiol* 551, 467–478.
Cadot B, Gache V, Vasyutina E, Falcone S, Birchmeier C, Gomes ER (2012). Nuclear movement during myotube formation is microtubule and dynein dependent and is regulated by Cdc42, Par6 and Par3. *Nature* 13, 741–749.
Chang W, Folker ES, Worman HJ, Gundersen GG (2013). Emerin organizes actin flow for nuclear movement and centrosome orientation in migrating fibroblasts. *Mol Biol Cell* 24, 3869–3880.
D'Allessandro M, Hnia K, Gache V, Koch C, Gavrilidis C, Rodriguez D, Nicot A, Romero NB, Schwab Y, Gomes E, et al. (2015). Amphiphysin 2 orchestrates nucleus positioning and shape by linking the nuclear envelope to the actin and microtubule cytoskeleton. *Dev Cell* 35, 186–198.
Dialynas G, Speese S, Budnik V, Geyer PK, Walrath LL (2010). The role of *Drosophila* Lamin C in muscle function and gene expression. *Development* 137, 3067–3077.
Dubowitz V, Sewry CA (Eds.) (2007). Definition of pathological changes seen in muscle biopsies. In: *Muscle Biopsy: A Practical Approach*, London, UK: Elsevier Publishing, 231–358.
Elhanany-Tamir H, Yu YV, Shnyder M, Jain A, Welte M, Volk T (2012). Organelle positioning in muscles requires cooperation between two KASH proteins and microtubules. *J Cell Biol* 198, 833–846.
Espigat-Georget A, Dyachuk V, Chemin C, Emorine L, Merdes A (2016). Nuclear alignment in myotubes requires centrosome proteins recruited by nesprin-1. *J Cell Sci* 129, 4227–4237.
Falcone S, Roman W, Hnia K, Gache V, Didier N, Laine J, Aurade F, Marty I, Nishino I, Charlet-Berguerand N, et al. (2014). N-WASP is required for Amphiphysin-2/BIN1-dependent nuclear positioning and triad organization in skeletal muscle and is involved in the pathophysiology of centronuclear myopathy. *EMBO Mol Med* 6, 1455–1475.
Flucher BE, Takekura H, Franzini-Armstrong C (1993). Development of the excitation-contraction coupling apparatus in skeletal muscle: association of sarcoplasmic reticulum and transverse tubules with myofibrils. *Dev Biol* 160, 135–147.
Folker ES, Schulman VK, Baylies MK (2012). Muscle length and myonuclear position are independently regulated by distinct Dynein pathways. *Development* 139, 3827–3837.
Folker ES, Schulman VK, Baylies MK (2014). Translocating myonuclei have distinct leading and lagging edges that require kinesin and dynein. *Development* 141, 355–366.
Gepner J, Li M, Ludmann S, Kortas C, Boylan K, Iyadurai SJ, McGrail M, Hays TS (1996). Cytoplasmic dynein function is essential in *Drosophila melanogaster*. *Genetics* 142, 865–878.
Gundersen GG, Worman HJ (2013). Nuclear positioning. *Cell* 152, 1376–1389.
Jungbluth H, Zhou H, Sewry CA, Robb S, Treves S, Bitoun M, Guicheney P, Buj-Bello A, Bönnemann C, Muntoni F (2007). Centronuclear myopathy due to a de novo dominant mutation in the skeletal muscle ryanodine receptor (RYR1) gene. *Neuromuscul Disord* 17, 338–345.
Kim JH, Jin P, Duan R, Chen EH (2015). Mechanisms of myoblast fusion during muscle development. *Curr Opin Genet Dev* 32, 162–170.
Lattao R, Bonaccorsi S, Guan X, Wasserman SA, Gatti M (2011). Tubby-tagged balancers for the *Drosophila* X and second chromosomes. *Fly* 5, 369–370.
Liechti-Gallati S, Muller B, Grimm T, Kress W, Muller C, Boltshauser E, Moser H, Braga S (1991). X-linked centronuclear myopathy: mapping the gene to Xq28. *Neuromuscul Disord* 1, 239–245.
Louis M, Huber T, Benton R, Sakmar TP, Vosshall LB (2007). Bilateral olfactory sensory input enhances chemotaxis behavior. *Nat Neurosci* 11, 187–199.
Meinke P, Nguyen TD, Wehnert MS (2011). The LINC complex and human disease. *Biochem Soc Trans* 39, 1693–1697.
Metzger T, Gache V, Xu M, Cadot B, Folker ES, Richardson BE, Gomes ER, Baylies MK (2012). MAP and kinesin-dependent nuclear positioning is required for skeletal muscle function. *Nature* 484, 120–124.

- Richardson BE, Beckett K, Nowak SJ, Baylies MK (2007). SCAR/WAVE and Arp2/3 are crucial for cytoskeletal remodeling at the site of myoblast fusion. *Development* 134, 4357–4367.
- Salpingidou G, Smertenko A, Hausmanowa-Petrucewicz I, Hussey PJ, Hutchison CJ (2007). A novel role for the nuclear membrane protein emerin in association of the centrosome to the outer nuclear membrane. *J Cell Biol* 178, 897–904.
- Schulman VK, Folker ES, Rosen JN, Baylies MK (2014). Syd/JIP3 and JNK signaling are required for myonuclear positioning and muscle function. *PLoS Genet* 10, e1004880-15.
- Sewry CA, Brown SC, Mercuri E, Bonne G, Feng L, Camici G, Morris GE, Muntoni F (2001). Skeletal muscle pathology in autosomal dominant Emery-Dreifuss muscular dystrophy with lamin A/C mutations. *Neuro-pathol Appl Neurobiol* 27, 281–290.
- Spiro AJ, Shy GM, Gonatas NK (1966). Myotubular myopathy. Persistence of fetal muscle in an adolescent boy. *Arch Neurol* 14, 1–14.
- Starr DA, Han M (2002). Role of ANC-1 in tethering nuclei to the actin cytoskeleton. *Science* 298, 406–409.
- Tassin AM, Maro B, Bornens M (1985). Fate of microtubule-organizing centers during myogenesis in vitro. *J Cell Biol* 100, 35–46.
- Welte MA, Gross SP, Postner M, Block SM, Wieschaus EF (1998). Developmental regulation of vesicle transport in *Drosophila* embryos: forces and kinetics. *Cell* 92, 547–557.
- Wilson MH, Holzbaur ELF (2014). Nesprins anchor kinesin-1 motors to the nucleus to drive nuclear distribution in muscle cells. *Development* 142, 218–228.
- Zaal KJM, Reid E, Mousavi K, Zhang T, Mehta A, Bugnard E, Sartorelli V, Ralston E (2011). Who needs microtubules? Myogenic reorganization of MTOC, Golgi complex and ER exit sites persists despite lack of normal microtubule tracks. *PLoS One* 6, e29057–16.
- Zelhof AC, Bao H, Hardy RW, Razzaq A, Zhang B, Doe CQ (2001). *Drosophila* Amphiphysin is implicated in protein localization and membrane morphogenesis but not in synaptic vesicle endocytosis. *Development* 128, 5005–5015.
- Zhang J, Felder A, Liu Y, Guo LT, Lange S, Dalton ND, Gu Y, Peterson KL, Mizisin AP, Shelton GD, et al. (2009). Nesprin 1 is critical for nuclear positioning and anchorage. *Hum Mol Genet* 19, 329–341.
- Zhang Q, Bethmann C, Worth NF, Davies JD, Wasner C, Feuer A, Ragnauth CD, Yi Q, Mellad JA, Warren DT, et al. (2007). Nesprin-1 and -2 are involved in the pathogenesis of Emery Dreifuss muscular dystrophy and are critical for nuclear envelope integrity. *Hum Mol Genet* 16, 2816–2833.